Acta Mech 227, 2361–2376 (2016)
DOI 10.1007/s00707-016-1613-6

ORIGINAL PAPER

Yahong Zhou · Peijun Wei · Qiheng Tang

Continuum model of a one-dimensional lattice of metamaterials

Received: 19 July 2015 / Revised: 2 October 2015 / Published online: 30 April 2016

Abstract The continuum model of a one-dimensional crystal lattice of a metamaterial is studied in this paper. First, the dispersive relation of a lattice wave in a one-dimensional crystal lattice of metamaterial is established and compared with that of the classic material. Then, the continuous medium modeling of the metamaterial is studied. It leads to the classical continuum model, the strain gradient continuum model, and the nonlocal gradient continuum model based on different assumptions. The disadvantages of the classic continuum model and the gradient continuum model are discussed. The nonlocal gradient continuum model is derived based on the nonlocal assumption of a continuous displacement field. The stability of dispersive curves is guaranteed, and the conceptions of negative mass and infinite mass are also avoided. The dispersive curves which correspond to the three kinds of models are compared with those of a discrete crystal lattice of metamaterial. The disadvantages of the classic continuum model and the gradient continuum model and the appropriate selection of a nonlocal parameter in the nonlocal gradient continuum model are discussed based on the numerical results.

1 Introduction

Recently, the investigations on the metamaterial attract the attention of many researchers. The metamaterial includes mainly two groups, i.e. the electromagnetic metamaterial (EMM) and acoustic metamaterial (AM). The electromagnetic metamaterials are generally regarded as materials that exhibit unusual properties, for example, negative electric permittivity (ε), negative magnetic permeability (μ), and hence a negative refractive index, for instance, [3,13–16]. The acoustic metamaterials are generally regarded as materials which possess negative effective mass or negative effective modulus which have attracted many researchers to turn to this study, such as [2,7–10,17] . The unusual properties of a metamaterial which are not readily observed in natural materials result from the manmade microstructures that are embedded in host material. These manmade microstructures include the electric resonators, the magnetic resonators, and the mechanical resonators. The photonic crystal and the phononic crystal have also the periodical microstructure as the metamaterial. However, different from the photonic crystal and the phononic crystal based on the Bragg scattering effects, the metamaterial possesses unusual properties which are mainly based on the local resonance of resonator. In order to study the mechanical behavior of acoustic metamaterial, Zhou and Hu [18] presented a unified analytic model for the elastic metamaterial with effective material parameters. The effective material properties are derived directly from the averages of local momentum, stress, and strain defined in a single doubly coated sphere. The physical mechanism of the negative effective mass density, negative effective bulk modulus and

Y. Zhou · P. Wei
Department of Applied Mechanics, University of Sciences and Technology Beijing, Beijing 100083, China

P. Wei (✉) · Q. Tang
State Key Laboratory of Nonlinear Mechanics (LNM), Chinese Academy of Science, Beijing, China
E-mail: weipj@ustb.edu.cn

negative effective shear modulus were illustrated clearly. The negative effective mass density is induced by negative total momentum of the composite for a positive momentum excitation. The negative effective bulk modulus appears for composites with an increasing (decreasing) total volume under a compressive (tensile) stress. The negative effective shear modulus describes composites with axisymmetric deformation under an opposite axisymmetric loading. Milton and Willis [12] proposed the mass-in-mass discrete model of acoustic metamaterial. Their study showed that the effective mass should be represented by a second-order tensor and can be anisotropic and frequency-dependent. Huang et al. [5] studied the dispersive wave propagation in the mass-in-mass lattice system and compared to various equivalent models. It is found that, if the classical elastic continuum is used to represent the original mass-in-mass lattice system, the effective mass density becomes frequency dependent and may become negative for frequencies near the resonance frequency of the internal mass. Huang and Sun [4] studied the wave attenuation and energy transfer mechanisms of a metamaterial having a negative effective mass density based on the mass-in-mass system. It is found that most of the work done by the external force on the lattice system is stored by the internal mass if the forcing frequency is close to the local resonance frequency. Huang and Sun [6] further investigated the dispersion curves and the band gap structure of a multi-resonator mass-in-mass lattice system. The unit cell of the lattice system consists of three separate masses connected by linear springs. In order to establish an effective continuum model, Zhu et al. [19] presented a microstructure continuum model to represent elastic metamaterials and used this continuum model to study wave propagation and band gaps in elastic metamaterial. Liu et al. [11] further proposed the multi-displacement microstructure continuum model for modeling the anisotropic elastic metamaterial. By comparison of the wave dispersion curves predicted by the proposed model and the finite element simulation for both longitudinal and transverse shear waves, very good agreement was observed in both the acoustic and the optic modes. Metrikine and Askes (2002) presented some gradient elasticity models derived from a discrete microstructure. In their work, a new continualization method is proposed in which each higher-order stiffness term is accompanied by a higher-order inertia term. As such, the resulting models are dynamically consistent. Because the physically realistic behavior is obtained in statics and dynamics, their gradient elasticity models are superior to earlier gradient elasticity models in which there are no anomalies in the dynamic behavior.

In this paper, the dynamical theory of crystal lattice established by Born and Huang [1] is used to study the lattice wave propagation in the one-dimensional crystal lattice of a metamaterial. The classical mass-spring system is replaced by the mass-in-mass system. In order to establish an effective continuum model of metamaterial with micro-resonator to keep same dispersive properties with the crystal lattice of a metamaterial, the classic continuum model, multi-displacement continuum model, and some gradient continuum models are derived from the discrete lattice based on different assumptions. The dispersive curves of these gradient continuum models are compared with those of the crystal lattice of a metamaterial. The disadvantages of the classic continuum model, and the gradient continuum model are discussed. The stable nonlocal gradient continuum model is proposed, and the appropriate selection of the nonlocal parameter in the nonlocal gradient continuum model is also discussed based on the numerical results.

2 The classic continuum model and the effective mass

Consider a diatomic chain of metamaterial with infinite extension, as shown in Fig. 1. The mass of atoms of macro-material and micro-material is indicated by m_1 and m_2, respectively. The spring coefficient between the atoms of the macro-material and that between the atoms of macro-material and micro-material is indicated by K_1 and K_2, respectively. $u_1^{(j)}$ and $u_2^{(j)}$ are the displacements of atoms of the macro-material and micro-material, respectively. L is the lattice distance. The motion equation of nth atoms of macro-material and nth atoms of micro-material are

$$m_1\ddot{u}_1^{(n)} = K_1\left(u_1^{(n+1)} + u_1^{(n-1)} - 2u_1^{(n)}\right) + K_2\left(u_2^{(n)} - u_1^{(n)}\right), \tag{1.1}$$

$$m_2\ddot{u}_2^{(n)} = K_2\left(u_1^{(n)} - u_2^{(n)}\right) \tag{1.2}$$

The solutions of the lattice wave are of the form

$$u_1^{(n\pm j)} = B_1\exp(i(qnL \pm jqL - \omega t)), \tag{2.1}$$

$$u_2^{(n\pm j)} = B_2\exp(i(qnL \pm jqL - \omega t)). \tag{2.2}$$

B_1 and B_2 are the amplitudes of the lattice wave. q is the wave vector, and ω is the angular frequency.

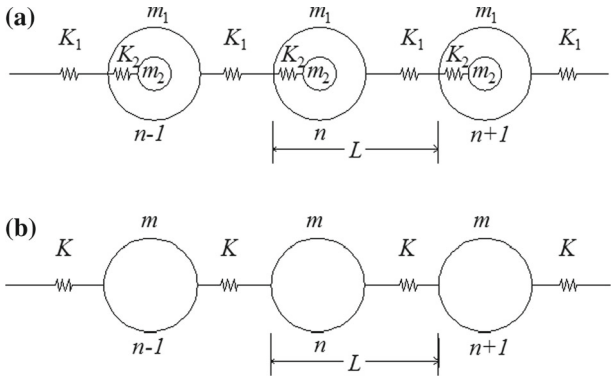

Fig. 1 Sketch of a one-dimensional diatomic chain of metamaterial. **a** Metamaterial crystal lattice with mass in mass; **b** simple lattice

Inserting Eq. (2) into Eq. (1) leads to

$$[m_1\omega^2 + K_1(e^{iqL} + e^{-iqL} - 2) - K_2]B_1 + K_2B_2 = 0, \tag{3.1}$$

$$K_2B_1 + (m_2\omega^2 - K_2)B_2 = 0. \tag{3.2}$$

The existence of a non-trivial solution requires that the coefficient determination is zero, i.e.

$$m_1m_2\omega^4 - [K_2m_1 + K_2m_2 + 2(1 - \cos(qL))K_1m_2]\omega^2 + 2K_1K_2(1 - \cos(qL)) = 0. \tag{4}$$

Equation (4) is the dispersive equation of the lattice wave in the one-dimensional crystal lattice of the metamaterial. Let $\alpha = m_2/m_1$, $\beta = K_2/K_1$, $\omega_0^2 = K_2/m_2$; then, the dispersive equation can be rewritten in the non-dimensional form as

$$\frac{\beta}{\alpha}\left(\frac{\omega}{\omega_0}\right)^4 - \left[\frac{\beta}{\alpha} + \beta + 2(1 - \cos(qL))\right]\left(\frac{\omega}{\omega_0}\right)^2 + 2\,(1 - \cos(qL)) = 0. \tag{5}$$

If $K_2 = 0$ and $m_2 = 0$, then, the crystal lattice of the metamaterial reduces to that of a classical material, and the dispersive equation reduces to

$$\omega^2 = \frac{2K_1(1 - \cos(qL))}{m_1}. \tag{6}$$

Equation (6) is the dispersive equation of the lattice wave in a classic material.

If the crystal lattice of the metamaterial is replaced by the crystal lattice of a classic material, see Fig. 1b, the dispersive properties of the lattice wave of the metamaterial keep unchanged. The dynamical effective mass should be introduced to represent the effects of the micro-material. Let the effective mass be indicated by m_{eff}. Then, the dispersive equation of the equivalent monoatom chain is

$$\omega^2 = \frac{2K_1(1 - \cos(qL))}{m_{\text{eff}}}. \tag{7}$$

Inserting Eq. (7) into Eq. (4) leads to

$$m_{\text{eff}} = m_{\text{st}} + \frac{m_2(\omega/\omega_0)^2}{1 - (\omega/\omega_0)^2} \tag{8}$$

where $m_{\text{st}}(= m_1 + m_2)$ is the static effective mass and $\omega_0 = \sqrt{\frac{K_2}{m_2}}$ is the resonant frequency of the micro-mass. Once the effective mass is obtained, the classic continuum model of the crystal lattice of the metamaterial can be expressed as

$$\rho\ddot{u} - K_1L\frac{\partial^2 u}{\partial x^2} = 0 \tag{9}$$

where $\rho = \frac{m_{\text{eff}}}{L}$. It is found from Eq. (8) that the dynamical effective mass is frequency-dependent. Figure 2 shows the frequency-dependency of the effective mass. When the frequency tends to the resonant frequency

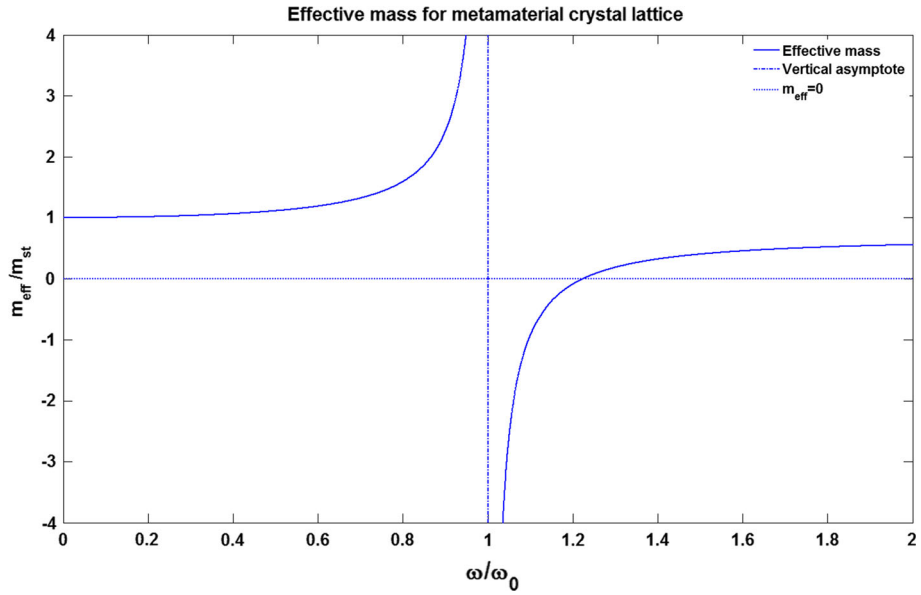

Fig. 2 The frequency-dependent effective mass $m_{\text{eff}}/m_{\text{st}}$

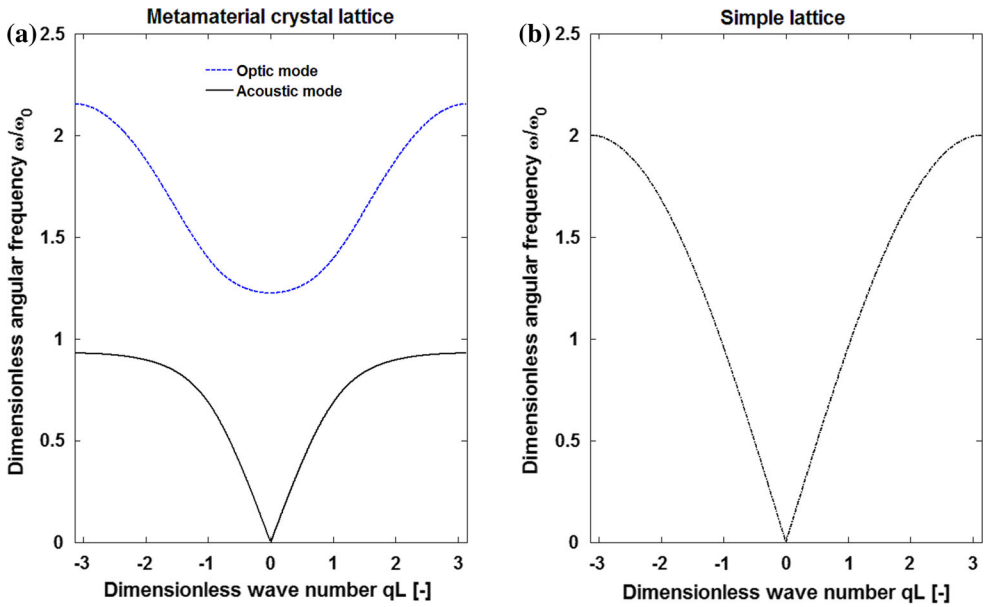

Fig. 3 The dispersion curves $\omega/\omega_0 - qL$. **a** Metamaterial crystal lattice with mass in mass ($m_2/m_1 = 0.5$, $K_2/K_1 = 0.5$, $\omega_0^2 = K_2/m_2$); **b** simple lattice ($m = m_1$, $K = K_1$, $\omega_0^2 = K_1/m_1$)

ω_0 from the left side ($\omega \leq \omega_0$), the effective mass becomes positive infinite. When the frequency tends to the resonant frequency ω_0 from the right side ($\omega \geq \omega_0$), the effective mass becomes negative infinite. This is an important feature of the metamaterial. Huang and Sun [4] gave a detailed investigation of the negative mass in the acoustic metamaterial and pointed out that the negative mass makes the wave number of the lattice wave become an imaginary number which means that the lattice wave is spatially decaying. In other word, the frequency which makes the effective mass negative falls into the stop band of a metamaterial. Because the negative mass always appears near the resonant frequency, the resonant frequency is thus an important parameter of metamaterial which represents the properties of the resonant microstructure.

Figure 3 shows the dispersive curves of a lattice wave in the crystal lattice of a metamaterial and in the simple crystal lattice of classic material. Different from the lattice wave in the classic material, the lattice wave

in the metamaterial has two branches. The acoustic branch is similar to that in the classic material but has lower frequency. The optical branch has higher frequency, and there is a band gap between the acoustic branch and the optical branch. This is similar to the dispersive curves of the diatom lattice in the classic material. But the optical branch for the metamaterial lattice is down concave, while the optical branch for classical material is upper convex. This makes the metamaterial easier to create the lower frequency band gap.

Figure 4 shows the influences of the mass ratio upon the dispersive curves, while Fig. 5 shows the influences of the rigidity ratio upon the dispersive curves. It is found that the increase of mass ratio makes the acoustic mode shift toward low frequency and the optical mode down concaving more evident. However, the increase of rigidity ratio has contrary influences when compared with the mass ratio. In other words, the mechanical resonator with larger mass and smaller rigidity is easier to create the low frequency bandgap.

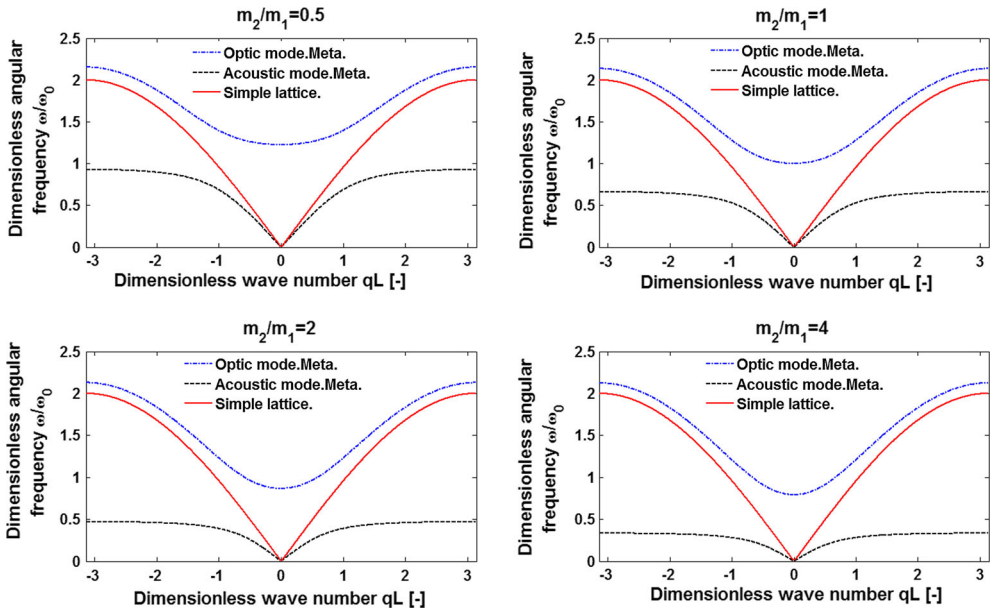

Fig. 4 The dispersion curves $\omega/\omega_0 - qL$ for different parameter ratios $m_2/m_1 (K_2/K_1 = 0.5,\ \omega_0^2 = K_2/m_2)$

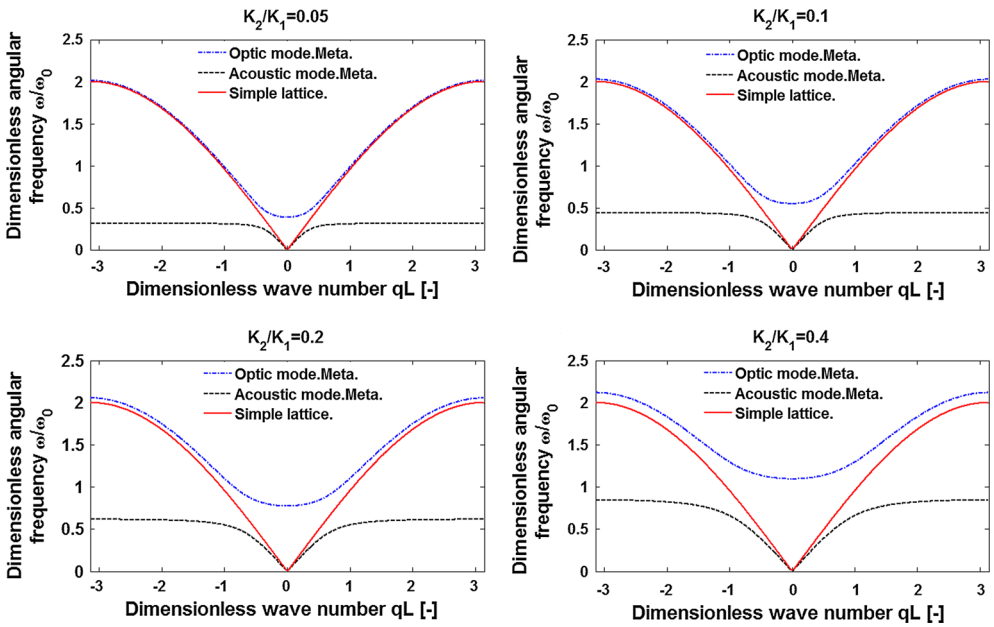

Fig. 5 The dispersion curves $\omega/\omega_0 - qL$ for different parameter ratios $K_2/K_1 (m_2/m_1 = 0.5,\ \omega_0^2 = K_2/m_2)$

3 Multi-displacement continuum model

The classic continuum representation of the metamaterial results in the frequency-dependent effective mass, and the effective mass can be negative or infinite. It is physically unacceptable. In order to overcome this disadvantage of the classic continuum model, Huang and Sun [4] proposed the multi-displacement continuum model. In the multi-displacement continuum model, two independent displacement fields, which correspond to the apparent mass and the hidden mass, are introduced, i.e.

$$u_1^{(n)}(t) = u_1(x,t), \tag{10.1}$$

$$u_2^{(n)}(t) = u_2(x,t). \tag{10.2}$$

The displacement of adjacent atoms can be expressed as

$$u_1^{(n+1)} = u_1(x+L) = u_1(x) + \frac{\partial u_1}{\partial x}L. \tag{11}$$

Then, the kinetic energy density and potential energy density can be expressed as

$$W = \frac{1}{2L}\left[K_1\left(u_1^{(n+1)} - u_1^{(n)}\right)^2 + K_2\left(u_2^{(n)} - u_1^{(n)}\right)^2\right] = \frac{1}{2L}\left[K_1(\varepsilon L)^2 + K_2\left(u_{12}L\right)^2\right], \tag{12.1}$$

$$T = \frac{1}{2L}\left[m_1\left(\dot{u}_1^{(n)}\right)^2 + m_2\left(\dot{u}_2^{(n)}\right)^2\right] \tag{12.2}$$

where $\varepsilon = \partial u_1/\partial x$ and $u_{12}(x) = (u_2 - u_1)/L$. Define the stress and the relative stress

$$\sigma = \frac{\partial W}{\partial \varepsilon} = LK_1\varepsilon = E\varepsilon, \tag{13.1}$$

$$\sigma_{12} = \frac{\partial W}{\partial u_{12}} = LK_2u_{12} = E_{12}u_{12}. \tag{13.2}$$

Equation (13) is the constitutive relation in the multi-displacement continuum model. By the application of the Hamilton variation principle,

$$\delta\int_{t_0}^{t_1}\int_V (T-W)\mathrm{d}V\mathrm{d}t + \int_{t_0}^{t_1}\int_S T_i\delta u_i\mathrm{d}A\mathrm{d}t = 0,$$

the motion equation can be expressed as

$$\rho_0\ddot{u}_1 + m_2\ddot{u}_{12} - K_1L\frac{\partial^2 u_1}{\partial x^2} = 0, \tag{14.1}$$

$$m_2L\ddot{u}_{12} + m_2\ddot{u}_1 + K_2Lu_{12} = 0 \tag{14.2}$$

where $\rho_0 = \frac{m_1+m_2}{L}$. Let

$$u_1 = A_1\exp(i(qx-\omega t)), \tag{15.1}$$

$$u_{12} = A_2\exp(i(qx-\omega t)). \tag{15.2}$$

And inserting them into Eq. (14), we can obtain the dispersive equation of wave propagation in the multi-displacement continuum model,

$$\frac{\beta}{\alpha}\left(\frac{\omega}{\omega_0}\right)^4 - \left[\frac{\beta}{\alpha} + \beta + (qL)^2\right]\left(\frac{\omega}{\omega_0}\right)^2 + (qL)^2 = 0. \tag{16}$$

Figure 6 shows the dispersive curves predicted by the multi-displacement continuum model. It is found that the dispersive curves of the acoustic mode predicted by the multiple displacement continuum model have good agreement with those predicted by the discrete crystal lattice model. But the dispersive curves of the optical mode predicted by the multiple displacement continuum model have good agreement with those predicted by the discrete crystal lattice model only at long wavelength range (near $qL = 0$). The deviation increases gradually as the wavelength decreases gradually.

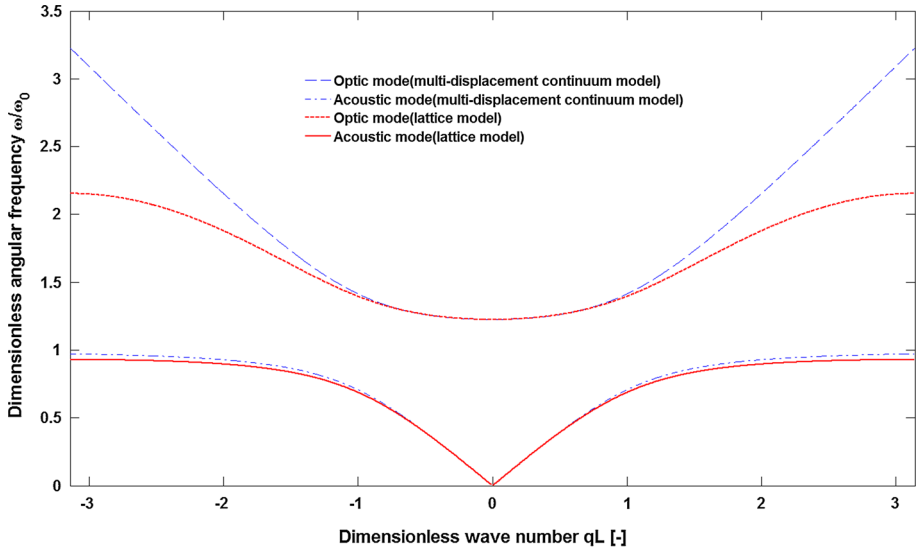

Fig. 6 The dispersion curves $\omega/\omega_0 - qL$ for the metamaterial crystal lattice model and the multi-displacement continuum model ($K_2/K_1 = 0.5$, $m_2/m_1 = 0.5$, $\omega_0^2 = K_2/m_2$)

4 Gradient continuum model

Let Eq. (11) be replaced by

$$u_1(x \pm L, t) = u_1 \pm Lu_{1,x} + \frac{1}{2!}L^2 u_{1,xx} \pm \frac{1}{3!}L^3 u_{1,xxx} + \frac{1}{4!}L^4 u_{1,xxxx} \pm \frac{1}{5!}L^5 u_{1,xxxxx} + \cdots \tag{17}$$

Inserting Eqs. (10) and (17) into Eq. (1) leads to

$$m_1 \ddot{u}_1 = K_1 \mathrm{L}^2 \left(u_{1,xx} + \frac{1}{12}\mathrm{L}^2 u_{1,xxxx} + \frac{1}{360}\mathrm{L}^4 u_{1,xxxxxx} + \cdots \right) + K_2(u_2 - u_1), \tag{18.1}$$

$$m_2 \ddot{u}_2 = K_2(u_1 - u_2). \tag{18.2}$$

Recall that the one-dimensional motion equation in the classicity elasticity theory is

$$\rho \ddot{u}_1 = \frac{\partial \sigma}{\partial x}. \tag{19}$$

Equation (18.1) implies

$$\sigma = K \left(\varepsilon + \frac{1}{12}\mathrm{L}^2 \frac{\partial^2 \varepsilon}{\partial x^2} + \frac{1}{360}\mathrm{L}^4 \frac{\partial^4 \varepsilon}{\partial x^4} + \cdots \right) + K_0 \frac{1}{L} \int u_{12} \mathrm{d}x \tag{20}$$

where $K = \frac{\rho K_1 L^2}{m_1}$, $K_0 = \frac{\rho K_2 L^2}{m_1}$, $\rho = \frac{m_{\mathrm{eff}}}{L}$. Namely, the stress is dependent upon not only the strain but also the strain gradient. This is the essence of the strain gradient elasticity theory. It should be pointed that only the strain gradients of even order appear in Eq. (20). When Eq. (17) is truncated by the sixth order derivative, then the motion equation can be expressed as

$$m_1 \ddot{u}_1 = K_1 \mathrm{L}^2 \left(u_{1,xx} + \frac{1}{12}\mathrm{L}^2 u_{1,xxxx} + \frac{1}{360}\mathrm{L}^4 u_{1,xxxxxx} \right) + K_2(u_2 - u_1), \tag{21.1}$$

$$m_2 \ddot{u}_2 = K_2(u_1 - u_2). \tag{21.2}$$

Let

$$u_1 = C_1 \exp(i(qx - \omega t)), \tag{22.1}$$

$$u_2 = C_2 \exp(i(qx - \omega t)). \tag{22.2}$$

Inserting Eq. (22) into Eq. (21) leads to the dispersive equation

$$\omega^2 = \frac{(m_1 K_2 + m_2 \lambda_1(qL)) \pm \sqrt{\lambda_2(qL)}}{2m_1 m_2} \tag{23}$$

where

$$\lambda_1 = K_1 L^2 q^2 - \frac{1}{12} K_1 L^4 q^4 + \frac{1}{360} K_1 L^6 q^6 + K_2,$$
$$\lambda_2 = (m_1 K_2 + m_2 \lambda_1)^2 - 4m_1 m_2 (\lambda_1 K_2 - K_2^2).$$

Also, the dispersive equation can be rewritten in non-dimensional form as

$$\frac{\beta}{\alpha}\left(\frac{\omega}{\omega_0}\right)^4 - \left[\frac{\beta}{\alpha} + \beta + (qL)^2 - \frac{1}{12}(qL)^4 + \frac{1}{360}(qL)^6\right]\left(\frac{\omega}{\omega_0}\right)^2 + (qL)^2 - \frac{1}{12}(qL)^4 + \frac{1}{360}(qL)^6 = 0. \tag{24}$$

The dispersive curves corresponding to the gradient continuum model are shown in Figs. 7 and 8. It is found that the dispersive curves predicted by the gradient continuum model approximate satisfyingly those predicted by the discrete lattice model in a wider frequency range compared with the multiple displacement continuum model. The higher is the order of strain gradient included, the wider is the fitting frequency range. However, it is noted that the group speed of the acoustic mode tends to negative infinity as the wavelength decreases gradually, namely, $\lim_{q \to q_{cr}} c_g(q) = -\infty$, for the second, sixth and tenth order of gradient continuum models. This implies that the wave with wavelength smaller than $\lambda_{cr} = 2\pi/q_{cr}$ cannot propagate in the continuum medium. This is physically not realistic. On the other hand, the group speeds corresponding to fourth, eighth and twelfth order of the gradient continuum model are

$$c_g = \mathrm{d}\omega/\mathrm{d}q = \frac{\lambda_4(q^{11})}{\lambda_5(q^9)} \tag{25}$$

where

$$\lambda_3 = \frac{(m_1 K_2 + m_2 \lambda_1) \pm \sqrt{\lambda_2}}{2m_1 m_2},$$
$$\lambda_4(\mathrm{q}^{11}) = 2m_2\sqrt{\lambda_2}\frac{d\lambda_1}{dq} \pm \frac{d\lambda_2}{dq} \sim P_{11}(q),$$
$$\lambda_5(\mathrm{q}^9) = 8m_1 m_2 \sqrt{\lambda_2 \lambda_3} \sim P_9(q).$$

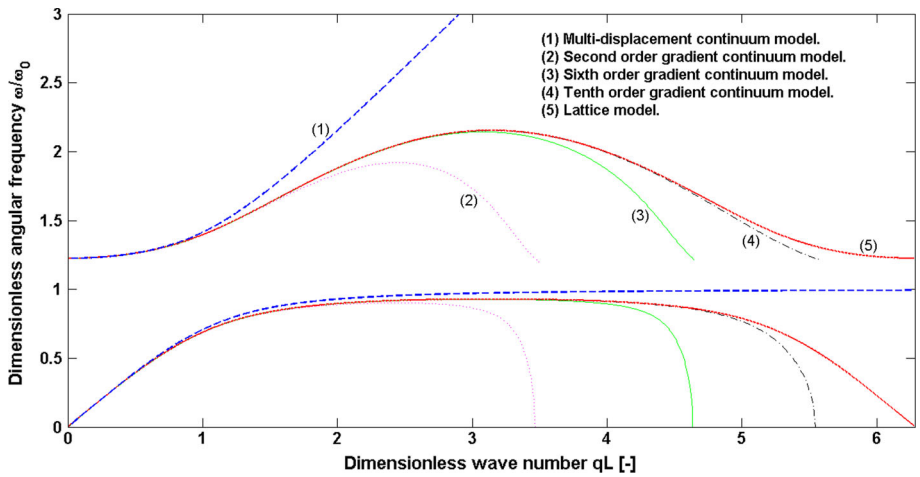

Fig. 7 The dispersion curves $\omega/\omega_0 - qL$ for some order of gradient continuum models compared with the lattice model and the multi-displacement continuum model ($K_2/K_1 = 0.5$, $m_2/m_1 = 0.5$, $\omega_0^2 = K_2/m_2$)

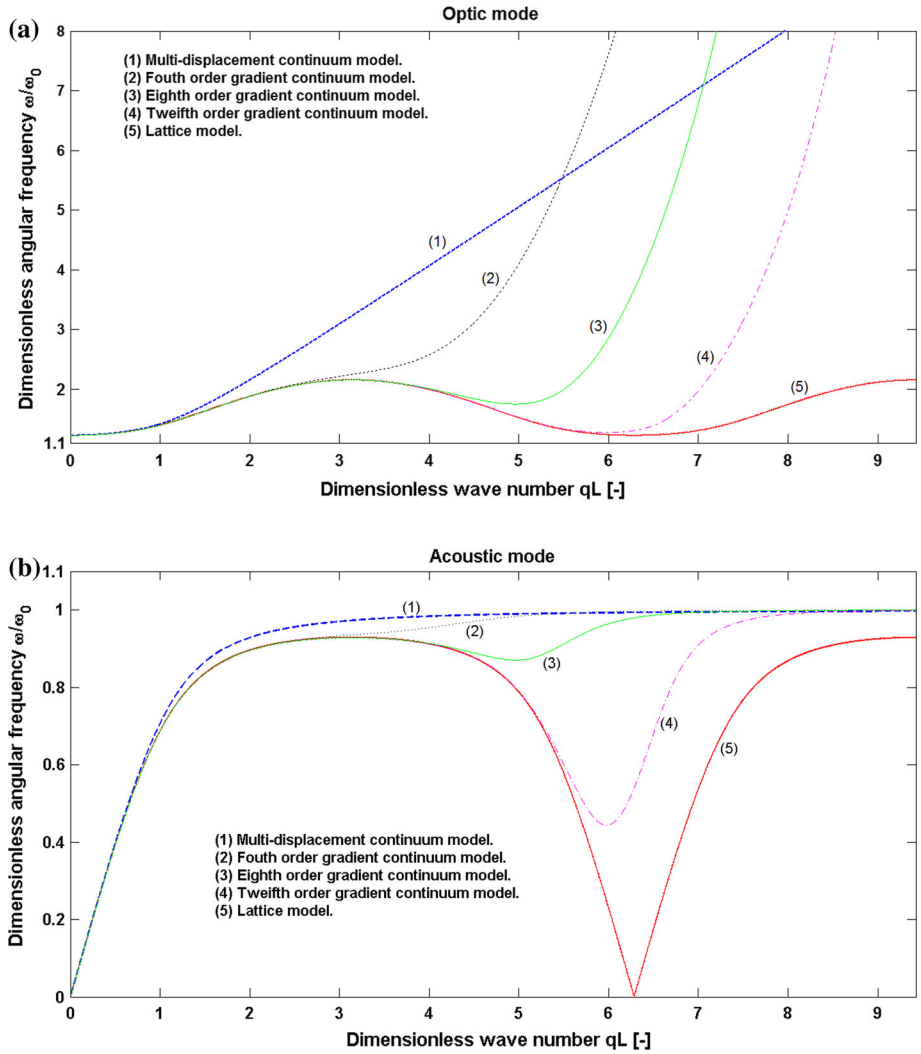

Fig. 8 The dispersion curves $\omega/\omega_0 - qL$ for some order of gradient continuum models compared with the lattice model and the multi-displacement continuum model. **a** The optic mode; **b** the acoustic mode ($K_2/K_1 = 0.5,\ m_2/m_1 = 0.5,\ \omega_0^2 = K_2/m_2$)

It is noted that $\lim_{q\to\infty} c_g(q) = \infty$ for the fourth, eighth and twelfth order of gradient continuum model. This implies that the speed at which the energy transmits tends to infinity as the frequency increases. This is also not realistic physically.

5 Nonlocal gradient continuum model

Instead of Eq. (10), let

$$u_1(x,t) = \frac{1}{1+2a_1+b_1}\left\{a_1 u_1^{(n-1)}(t) + u_1^{(n)}(t) + b_1 u_2^{(n)}(t) + a_1 u_1^{(n+1)}(t)\right\}, \tag{26.1}$$

$$u_2(x,t) = \frac{1}{1+c_1}\left\{u_2^{(n)}(t) + c_1 u_1^{(n)}(t)\right\}. \tag{26.2}$$

It means that the continuous displacement fields $u_1(x,t)$ and $u_2(x,t)$ are the averaged values of the displacements of adjacent several atoms. The parameters a_1, b_1, and c_1 are the weighting coefficients. These weighting coefficients satisfy $0 \le a_1 < 1$, $0 \le b_1 < 1$, and $0 \le c_1 < 1$. The nonlocal effects are taken into account when the continuous displacement field $u_1(x,t)$ and $u_2(x,t)$ is established by Eq. (26). Mathematically, this implies

that the displacement in a point after the continualization is not only related to the displacement in the same point but also instantly to the displacement in the neighboring points. Physically, it is a natural consequence of assigning the properties of a finite volume of inhomogeneous material to a point.

In order to obtain the motion equation with respective to displacement $u_1(x,t)$ and $u_2(x,t)$, we should express $u_1^{(n)}(t)$, $u_1^{(n\pm1)}(t)$, and $u_2^{(n)}(t)$ in terms of the continuous field $u_1(x,t)$, $u_2(x,t)$and their derivatives. We assume that the deviations of $u_1^{(n)}(t)$ from $u_1(x,t)$ and $u_2^{(n)}(t)$ from $u_2(x,t)$ are both small, so that the following relationship may be written:

$$u_1^{(n)}(t) = u_1(x,t) + \sum_{j=1}^{2N} L^j f_j(x,t) + O(L^{2N+1}), \tag{27.1}$$

$$u_2^{(n)}(t) = u_2(x,t) + \sum_{j=1}^{2N} L^j g_j(x,t) + O(L^{2N+1}). \tag{27.2}$$

In order to ensure the convergence of these series, the following condition is required:

$$L^{j+1} f_{j+1}(x,t) \ll L^j f_j(x,t),\ L^{j+1} g_{j+1}(x,t) \ll L^j g_j(x,t).$$

These functions of $f_j(x,t)$ and $g_j(x,t)$ are unknown and should be determined by inserting those discrete displacements into Eq. (26). The displacement of an adjacent point can be obtained by the application of the Taylor expansions

$$\begin{aligned} u_1^{(n\pm1)}(t) &= u_1(x \pm L, t) + \sum_{j=1}^{2N} L^j f_j(x \pm L, t) + O(L^{2N+1}) \\ &= \sum_{m=0}^{2N} (\pm1)^m \frac{L^m}{m!} \frac{\partial^m u_1(x,t)}{\partial x^m} + \sum_{m=0}^{2N} \sum_{j=1}^{2N-m} (\pm1)^m \frac{L^{m+j}}{m!} \frac{\partial^m f_j(x,t)}{\partial x^m} + O(L^{2N+1}). \end{aligned} \tag{28}$$

Inserting Eqs. (27) and (28) into Eq. (26) leads to

$$\begin{aligned} u_1(x,t) = {} & \frac{1}{1+2a_1+b_1} \left(u_1(x,t) + \sum_{j=1}^{2N} L^j f_j(x,t) \right) + \frac{2a_1}{1+2a_1+b_1} \sum_{m=0}^{N} \frac{L^{2m}}{(2m)!} \frac{\partial^{2m} u_1(x,t)}{\partial x^{2m}} \\ & + \frac{2a_1}{1+2a_1+b_1} \sum_{m=0}^{N} \sum_{j=1}^{2N-2m} \frac{L^{2m+j}}{(2m)!} \frac{\partial^{2m} f_j(x,t)}{\partial x^{2m}} + \frac{b_1}{1+2a_1+b_1} u_2(x,t) \\ & + \frac{b_1}{1+2a_1+b_1} \sum_{j=1}^{2N} L^j g_j(x,t) + O(L^{2N+1}), \end{aligned} \tag{29.1}$$

$$u_2(x,t) = \frac{1}{c_1} \sum_{j=1}^{2N} L^j g_j(x,t) + u_1(x,t) + \sum_{j=1}^{2N} L^j f_j(x,t) + O(L^{2N+1}). \tag{29.2}$$

Further, inserting Eq. (29.2) into Eq. (29.1), we obtain

$$\begin{aligned} u_1(x,t) = {} & \frac{1+b_1}{1+2a_1+b_1} \left(u_1(x,t) + \sum_{j=1}^{2N} L^j f_j(x,t) \right) + \frac{2a_1}{1+2a_1+b_1} \sum_{m=0}^{N} \frac{L^{2m}}{(2m)!} \frac{\partial^{2m} u_1(x,t)}{\partial x^{2m}} \\ & + \frac{2a_1}{1+2a_1+b_1} \sum_{m=0}^{N} \sum_{j=1}^{2N-2m} \frac{L^{2m+j}}{(2m)!} \frac{\partial^{2m} f_j(x,t)}{\partial x^{2m}} + \frac{b_1}{1+2a_1+b_1} \frac{c_1+1}{c_1} \sum_{j=1}^{2N} L^j g_j(x,t) \\ & + O(L^{2N+1}). \end{aligned} \tag{30}$$

It is assumed that the operator $L\partial/\partial x$ be much smaller than unity, so we may consider Eq. (30) by using the perturbation method. By comparing the coefficients of L^n at both sides of equal mark, we obtain the following set of equations, ordered by the corresponding powers of L^n:

$$L^0: \quad u_1 = \frac{1}{1+2a_1+b_1}(u_1 + 2a_1u_1 + b_1u_1), \tag{31.1}$$

$$L^1: \quad 0 = (1+2a_1+b_1)f_1 + \left(1+\frac{1}{c_1}\right)b_1g_1, \tag{31.2}$$

$$L^2: \quad 0 = (1+2a_1+b_1)f_2 + \left(1+\frac{1}{c_1}\right)b_1g_2 + a_1\frac{\partial^2 u_1}{\partial x^2}, \tag{31.3}$$

$$L^3: \quad 0 = (1+2a_1+b_1)f_3 + \left(1+\frac{1}{c_1}\right)b_1g_3 + a_1\frac{\partial^2 f_1}{\partial x^2}, \tag{31.4}$$

$$L^4: \quad 0 = (1+2a_1+b_1)f_4 + \left(1+\frac{1}{c_1}\right)b_1g_4 + \frac{a_1}{12}\frac{\partial^4 u_1}{\partial x^4} + a_1\frac{\partial^2 f_2}{\partial x^2}, \tag{31.5}$$

$$L^5: \quad 0 = (1+2a_1+b_1)f_5 + \left(1+\frac{1}{c_1}\right)b_1g_5 + \frac{a_1}{12}\frac{\partial^4 f_1}{\partial x^4} + a_1\frac{\partial^2 f_3}{\partial x^2}, \tag{31.6}$$

$$L^6: \quad 0 = (1+2a_1+b_1)f_6 + \left(1+\frac{1}{c_1}\right)b_1g_6 + \frac{a_1}{360}\frac{\partial^6 u_1}{\partial x^6} + \frac{a_1}{12}\frac{\partial^4 f_2}{\partial x^4} + a_1\frac{\partial^2 f_4}{\partial x^2} \tag{31.7}$$

which can be generalized as

$$L^m(\mathrm{m}=1,3,5,\ldots): \quad 0 = (1+b_1)f_m + 2a_1\sum_{j=0}^{(\mathrm{m}-1)/2}\frac{1}{(2j)!}\frac{\partial^{2j} f_{m-2j}(x,t)}{\partial x^{2j}}, \tag{32.1}$$

$$\begin{aligned} L^m(\mathrm{m}=2,4,6,\ldots): \quad 0 &= (1+b_1)f_m + 2a_1\frac{1}{(m)!}\frac{\partial^m u_1(x,t)}{\partial x^m} \\ &\quad + 2a_1\sum_{j=0}^{m/2-1}\frac{1}{(2j)!}\frac{\partial^{2j} f_{m-2j}(x,t)}{\partial x^{2j}}. \end{aligned} \tag{32.2}$$

Equation (31.1) is satisfied automatically. By observation of odd power of L, it is found that $f_j(j = 1,3,5,\ldots) = 0$ and $g_j(j = 1,3,5,\ldots) = 0$. By observation of an even power of L, it is found that $g_j(j = 2,4,6,\ldots) = 0$, and

$$f_2 = -\frac{a_1}{1+2a_1+b_1}\frac{\partial^2 u_1}{\partial x^2}, \tag{33.1}$$

$$f_4 = \frac{a_1(10a_1-1-b_1)}{12(1+2a_1+b_1)^2}\frac{\partial^4 u_1}{\partial x^4}, \tag{33.2}$$

$$f_6 = -\frac{a_1(1-56a_1-56a_1b_1+2b_1+244a_1^2+b_1^2)}{360(1+2a_1+b_1)^3}\frac{\partial^6 u_1}{\partial x^6}. \tag{33.3}$$

After f_j and g_j are determined, the expressions of the discrete displacements $u_1^{(n)}(t)$, $u_2^{(n)}(t)$, and $u_1^{(n\pm1)}(t)$ in terms of the continuous displacement field $u_1(x,t)$and $u_2(x,t)$ are obtained. Inserting them into the motion equation of the discrete lattice of the metamaterial, i.e. Eq. (1), we obtain

$$\begin{aligned} &m_1\left(\frac{\partial^2 u_1(x,t)}{\partial t^2} + \sum_{m=1}^{M} L^{2m}\frac{\partial^2 f_{2m}(x,t)}{\partial t^2}\right) + 2K_1\left(u_1(x,t) + \sum_{m=1}^{M} L^{2m} f_{2m}(x,t)\right) \\ &- 2K_1\left(\sum_{m=0}^{M}\frac{L^{2m}}{(2m)!}\frac{\partial^{2m} u_1(x,t)}{\partial x^{2m}} + \sum_{m=0}^{M}\sum_{j=1}^{M-m}\frac{L^{2(m+j)}}{(2m)!}\frac{\partial^{2m} f_{2j}(x,t)}{\partial x^{2m}}\right) \\ &+ K_2\left(u_1(x,t) + \sum_{m=1}^{M} L^{2m} f_{2m}(x,t) - u_2(x,t)\right) = O(L^{2M+2}), \end{aligned} \tag{34.1}$$

$$m_2\frac{\partial^2 u_2(x,t)}{\partial t^2} + K_2\left(u_2(x,t) - u_1(x,t) - \sum_{m=1}^{M} L^{2m} f_{2m}(x,t)\right) = O(L^{2M+2}). \tag{34.2}$$

Truncating the infinite series in Eq. (34) by $M = 3$, we obtain

$$m_1\left(\frac{\partial^2 u_1}{\partial t^2}+L^2\frac{\partial^2 f_2}{\partial t^2}+L^4\frac{\partial^2 f_4}{\partial t^2}\right)-2K_1\left(\frac{L^2}{2}\frac{\partial^2 u_1}{\partial x^2}+\frac{L^4}{24}\frac{\partial^4 u_1}{\partial x^4}+\frac{L^6}{720}\frac{\partial^6 u_1}{\partial x^6}\right.$$
$$\left.+\frac{L^4}{2}\frac{\partial^2 f_2}{\partial x^2}+\frac{L^6}{2}\frac{\partial^2 f_4}{\partial x^2}+\frac{L^6}{24}\frac{\partial^4 f_2}{\partial x^4}\right)+K_2\left(u_1+L^2 f_2+L^4 f_4+L^6 f_6-u_2\right)=0, \tag{35.1}$$

$$m_2\frac{\partial^2 u_2}{\partial t^2}+K_2\left(u_2-u_1-L^2 f_2-L^4 f_4-L^6 f_6\right)=0. \tag{35.2}$$

After inserting the expressions of f_2, f_4 and f_6, we obtain

$$m_1\left(\frac{\partial^2 u_1}{\partial t^2}-d_1\frac{\partial^2 u_1}{\partial x^2}\right)-\frac{m_1 a_1 L^2}{1+2a_1+b_1}\frac{\partial^2}{\partial x^2}\left(\frac{\partial^2 u_1}{\partial t^2}-d_2\frac{\partial^2 u_1}{\partial x^2}\right)$$
$$+\frac{m_1 a_1(10a_1-1-b_1)L^4}{12(1+2a_1+b_1)^2}\frac{\partial^4}{\partial x^4}\left(\frac{\partial^2 u_1}{\partial t^2}-d_3\frac{\partial^2 u_1}{\partial x^2}\right)+K_2\left(u_1-u_2\right)=0, \tag{36.1}$$

$$m_2\frac{\partial^2 u_2}{\partial t^2}+h_1\frac{\partial^2 u_1}{\partial x^2}+h_2\frac{\partial^4 u_1}{\partial x^4}+h_3\frac{\partial^6 u_1}{\partial x^6}+K_2\left(u_2-u_1\right)=0. \tag{36.2}$$

Similarly, truncating the infinite series by $M = 2$, we obtain

$$m_1\left(\frac{\partial^2 u_1}{\partial t^2}-d_1\frac{\partial^2 u_1}{\partial x^2}\right)-\frac{m_1 a_1 L^2}{1+2a_1+b_1}\frac{\partial^2}{\partial x^2}\left(\frac{\partial^2 u_1}{\partial t^2}-d_2\frac{\partial^2 u_1}{\partial x^2}\right)+K_2\left(u_1-u_2\right)=0, \tag{37.1}$$

$$m_2\frac{\partial^2 u_2}{\partial t^2}+h_1\frac{\partial^2 u_1}{\partial x^2}+h_2\frac{\partial^4 u_1}{\partial x^4}+K_2\left(u_2-u_1\right)=0. \tag{37.2}$$

Let the solution be of form

$$u_1 = A\exp(i(qx-\omega t)), \tag{38.1}$$
$$u_2 = B\exp(i(qx-\omega t)). \tag{38.2}$$

Inserting Eq. (38) into Eq. (36) leads to

$$(-m_1\omega^2+m_1 d_1 q^2+s_1 q^2\omega^2-s_1 d_2 q^4-s_2 q^4\omega^2+s_2 d_3 q^6+K_2)A-K_2 B=0, \tag{39.1}$$
$$(-m_2\omega^2+K_2)B+(-h_1 q^2+h_2 q^4-h_3 q^6-K_2)A=0. \tag{39.2}$$

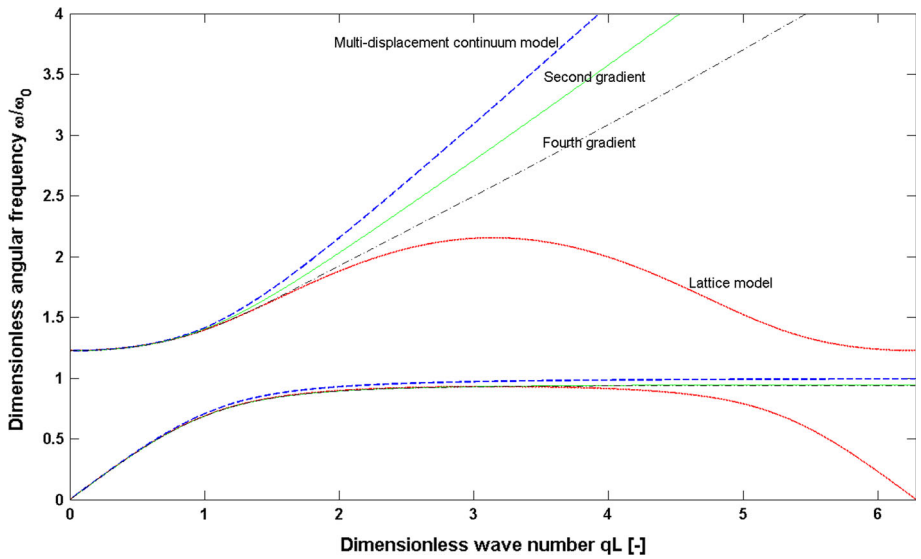

Fig. 9 The dispersion curves $\omega/\omega_0 - qL$ with $a_1 = 0.4, b_1 = 0$ for the second and the fourth nonlocal gradient continuum models compared with the lattice model and the multi-displacement continuum model ($K_2/K_1 = 0.5$, $m_2/m_1 = 0.5$, $\omega_0^2 = K_2/m_2$)

The dispersive equation is obtained by requiring the coefficient determinant to be equal to zero,

$$\begin{vmatrix} -\frac{\beta}{\alpha}\left(\frac{\omega}{\omega_0}\right)^2 + \gamma_1\cdot(\mathrm{qL})^2 - \gamma_2\cdot(\mathrm{qL})^2\frac{\beta}{\alpha}(\frac{\omega}{\omega_0})^2 + \gamma_3\cdot(\mathrm{qL})^4 - \gamma_4\cdot(\mathrm{qL})^4\frac{\beta}{\alpha}(\frac{\omega}{\omega_0})^4 + \gamma_5\cdot(\mathrm{qL})^6 + \beta & -\beta \\ \gamma_6\cdot(\mathrm{qL})^2 + \gamma_7\cdot(\mathrm{qL})^4 + \gamma_8\cdot(\mathrm{qL})^6 - 1 & -\left(\frac{\omega}{\omega_0}\right)^2 + 1 \end{vmatrix} = 0. \tag{40}$$

Similarly, the dispersive equation corresponding to Eq. (37) is

$$\begin{vmatrix} -\frac{\beta}{\alpha}\left(\frac{\omega}{\omega_0}\right)^2 + \gamma_1\cdot(\mathrm{qL})^2 - \gamma_2\cdot(\mathrm{qL})^2\frac{\beta}{\alpha}(\frac{\omega}{\omega_0})^2 + \gamma_3\cdot(\mathrm{qL})^4 + \beta & -\beta \\ \gamma_6\cdot(\mathrm{qL})^2 + \gamma_7\cdot(\mathrm{qL})^4 - 1 & -\left(\frac{\omega}{\omega_0}\right)^2 + 1 \end{vmatrix} = 0 \tag{41}$$

where the explicit expressions of d_i, h_i, s_i and γ_i are given in the "Appendix" .

The dispersive curves corresponding to the nonlocal gradient continuum model are shown in Fig. 9. It is observed that the dispersive curves predicted by the nonlocal gradient continuum model can match those predicted by the discrete lattice model in a wider frequency range compared with the multiple displacement

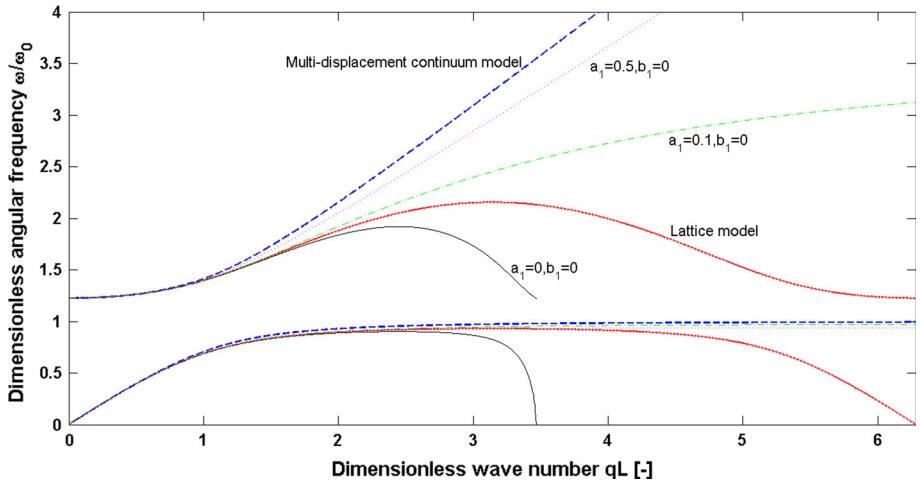

Fig. 10 The effect of a_1 on the dispersion curves $\omega/\omega_0 - qL$ for the second nonlocal gradient continuum model compared with the lattice model and the multi-displacement continuum model ($K_2/K_1 = 0.5$, $m_2/m_1 = 0.5$, $\omega_0^2 = K_2/m_2$)

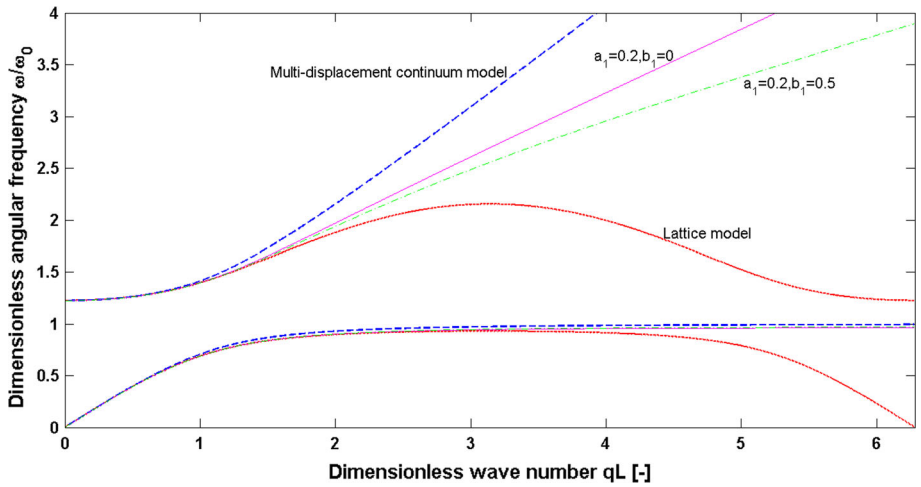

Fig. 11 The effect of b_1 on the dispersion curves $\omega/\omega_0 - qL$ for the second nonlocal gradient continuum model which is compared with the lattice model and the multi-displacement continuum model ($K_2/K_1 = 0.5$, $m_2/m_1 = 0.5$, $\omega_0^2 = K_2/m_2$)

continuum model. The higher the order of the nonlocal gradient continuum model, the better the dispersive curves fit. Compared with the gradient continuum model, there are two nonlocal parameters, a_1 and b_1, in the nonlocal gradient continuum model. By adjusting the two nonlocal parameters, the unconditionally stable dispersive curves can be obtained. Figures 10 and 12 show the effects of the nonlocal parameter a_1 on the dispersive curves. It is observed that the increase of a_1 helps to get stable dispersive curves. If the nonlocal parameter a_1 is not enough larger, the acoustic mode in the second nonlocal gradient continuum model will attenuate in advance, while the optical mode in the fourth nonlocal gradient continuum model will have infinite speed of energy transmission. Figures 11 and 13 show the effects of the nonlocal parameter b_1 on the dispersive curves. It is observed that the increase of the nonlocal parameter b_1 always make the dispersive curves better fitting those given by the discrete lattice model. Although the two parameters, a_1 and b_1, can improve the dispersive curves predicted by the nonlocal gradient continuum model, their contributions are different. The nonlocal parameter a_1 plays a more important role than the nonlocal parameter b_1. If the nonlocal parameter a_1 satisfies $0 \leq a_1 < 0.1$ in the second gradient and $0 \leq a_1 < 0.25$ in the fourth gradient, the acoustic

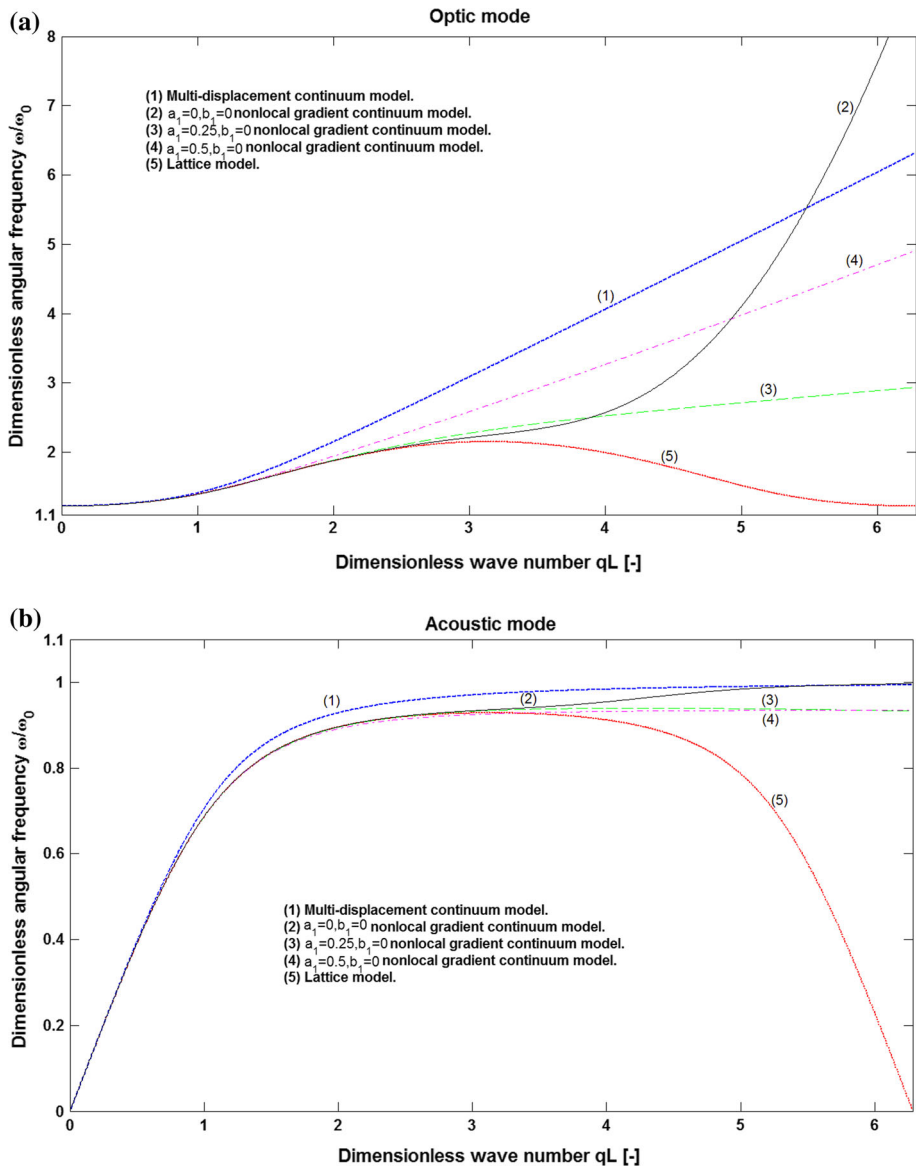

Fig. 12 The effect of a_1 on the dispersion curves $\omega/\omega_0 - qL$ for the fourth nonlocal gradient continuum model compared with the lattice model and the multi-displacement continuum model ($K_2/K_1 = 0.5$, $m_2/m_1 = 0.5$, $\omega_0^2 = K_2/m_2$). **a** The optic mode; **b** the acoustic mode

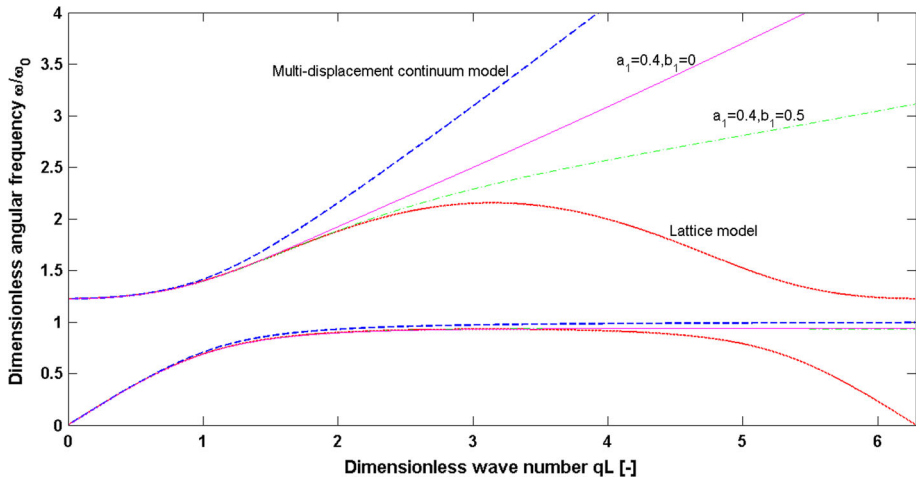

Fig. 13 The effect of b_1 on the dispersion curves $\omega/\omega_0 - qL$ for the fourth nonlocal gradient continuum model compared with the lattice model and the multi-displacement continuum model ($K_2/K_1 = 0.5$, $m_2/m_1 = 0.5$, $\omega_0^2 = K_2/m_2$)

mode attenuates in advance whether the nonlocal parameter b_1 takes which value. On the other hand, if the nonlocal parameter a_1 satisfies $a_1 \geq 0.2$ in the second nonlocal gradient model and $a_1 \geq 0.5$ in the fourth nonlocal gradient model, the dispersive curves are always stable whether b_1 take which value. Therefore, the nonlocal parameter a_1 mainly guarantees the stability of the dispersive curves, while the nonlocal parameter b_1 mainly improves the precision of the dispersive curves. In particular, when $a_1 = 0$ and $b_1 = 0$, the higher-order dynamical consistent terms, $s_1\partial^4 u_1/\partial x^2\partial t^2$ in the second nonlocal gradient model, and $s_1\partial^4 u_1/\partial x^2\partial t^2$, $s_2\partial^6 u_1/\partial x^4\partial t^2$ in the fourth nonlocal gradient model, vanish, and the nonlocal gradient model reduces to the local gradient model in Sect. 4.

6 Conclusions

The unique nature of the acoustic metamaterial is the existence of a local resonator compared with the classic elastic material. The appropriate representation of the crystal lattice of a metamaterial is the mass-in-mass plus spring system. The dispersive curves of the lattice wave in a crystal lattice of metamaterial have a low frequency band gap between the acoustic mode and the optical mode which is different from that in the monoatom chain and diatom chain of a classic material. Some continuum models are studied in the present work, and some conclusions can be drawn as follows:

1. The classical continuum model of a discrete lattice cannot predict the low frequency bandgap because only a single acoustic branch is predicted. In order to predict the low frequency band gap of a metamaterial, the classic continuum model results in the frequency-dependent negative effective mass and the infinite mass at the certain frequency which is physically unacceptable.
2. The multiple displacement continuum model introduces an additional degree of freedom of micro-motion and thus predicts not only the low frequency band gap but also avoids the introduction of negative mass and infinite mass. The acoustic branch predicted by the multiple displacement continuum model has good agreement with that of the lattice mode. However, the optical branch has good agreement with that of the lattice model only for an elastic wave with long wavelength ($qL < 1$). The deviation increases evidently as the wavelength decreases.
3. The gradient continuum model can evidently improve the prediction decision and the applied frequency range of the multiple displacement continuum model. But the dispersive curves predicted are not unconditionally stable.
4. The nonlocal gradient continuum model takes the nonlocal effects into consideration when establishing the continuous displacement field from the discrete displacement of adjacent atoms. By appropriate selection of the nonlocal parameter, the nonlocal gradient continuum model is unconditionally stable and can predict physically realistic dispersive curves at the total frequency range.

Acknowledgments The work is supported by the National Natural Science Foundation of China (No. 10972029) and Opening fund of State Key Laboratory of Nonlinear Mechanics (LNM).

Appendix

$$d_1 = \frac{K_1L^2}{m_1} + \frac{K_2L^2a_1}{m_1(1+2a_1+b_1)}, \quad d_2 = \frac{K_1L^2}{m_1} - \frac{K_1L^2(1+2a_1+b_1)}{12m_1a_1} + \frac{K_2L^2(10a_1-1-b_1)}{12m_1(1+2a_1+b_1)},$$

$$d_3 = \frac{K_1L^2}{m_1} - \frac{K_1L^2(1+2a_1+b_1)}{m_1(10a_1-1-b_1)} + \frac{K_1L^2(1+2a_1+b_1)^2}{30m_1a_1(10a_1-1-b_1)} + \frac{K_2L^2(1-56a_1-56a_1b_1+2b_1+244a_1^2+b_1^2)}{30m_1(1+2a_1+b_1)(10a_1-1-b_1)},$$

$$h_1 = \frac{K_2L^2a_1}{1+2a_1+b_1}, \quad h_2 = -\frac{K_2L^4a_1(10a_1-1-b_1)}{12(1+2a_1+b_1)^2}, \quad h_3 = \frac{K_2L^6a_1(1-56a_1-56a_1b_1+2b_1+244a_1^2+b_1^2)}{360(1+2a_1+b_1)^3},$$

$$s_1 = -\frac{m_1L^2a_1}{1+2a_1+b_1}, \quad s_2 = \frac{m_1L^4a_1(10a_1-1-b_1)}{12(1+2a_1+b_1)^2}, \quad \gamma_1 = \frac{1+(2+\beta)a_1+b_1}{1+2a_1+b_1}, \quad \gamma_2 = \frac{a_1}{1+2a_1+b_1},$$

$$\gamma_3 = \frac{(10a_1-1-b_1)[1+(2+\beta)a_1+b_1]}{12(1+2a_1+b_1)^2}, \quad \gamma_4 = \frac{a_1(10a_1-1-b_1)}{12(1+2a_1+b_1)^2},$$

$$\gamma_5 = \frac{(1-56a_1-56a_1b_1+2b_1+244a_1^2+b_1^2)[1+(2+\beta)a_1+b_1]}{360(1+2a_1+b_1)^3},$$

$$\gamma_6 = -\frac{a_1}{1+2a_1+b_1}, \quad \gamma_7 = -\frac{a_1(10a_1-1-b_1)}{12(1+2a_1+b_1)^2},$$

$$\gamma_8 = -\frac{a_1(1-56a_1-56a_1b_1+2b_1+244a_1^2+b_1^2)}{360(1+2a_1+b_1)^3}.$$

References

1. Born, M., Huang, K.: Dynamical Theory of Crystal Lattice. Oxford University Press, London (1954)
2. Fang, N., Xi, D., Xu, J., et al.: Ultrasonic metamaterial with negative modulus. Nat. Mater. **5**, 452–456 (2006)
3. Fang, F., Koschny, T., Soukoulis, C.M.: Optical anisotropic metamaterials: negative refraction and focusing. Phys. Rev. B **79**, 245127 (2009)
4. Huang, H., Sun, C.: Wave attenuation mechanism in an acoustic metamaterial with negative effective mass density. New J. Phys. **11**, 013003 (2009)
5. Huang, H., Sun, C., Huang, G.: On the negative effective mass density in acoustic metamaterials. Int. J. Eng. Sci. **47**, 610–617 (2009)
6. Huang, G., Sun, C.: Band gaps in a multiresonator acoustic metamaterial. J. Vib. Acoust. **132**, 031003 (2010)
7. Kadic, M., Bückmann, T., Stenger, N., Thiel, M., Wegener, M.: On the practicability of pentamode mechanical metamaterials. Appl. Phys. Lett. **100**, 191901 (2012)
8. Liu, Z.Y., Zhang, X.X., Mao, Y.W., et al.: Locally resonant sonic materials. Science **289**, 1734–1736 (2000)
9. Li, J., Chan, C.T.: Double-negative acoustic metamaterials. Phys. Rev. E **70**, 055602 (2004)
10. Lu, M.H., Fang, L., Chen, Y.F.: Phononic crystals and acoustic metamaterials. Mater. Today **12**, 34–42 (2009)
11. Liu, A.P., Zhu, R., Liu, X.N., et al.: Multi-displacement microstructure continuum modeling of anisotropic elastic metamaterials. Wave Motion **49**, 411–426 (2012)
12. Milton, G.W., Willis, J.R.: On modifications of Newton's second law and linear continuum elastodynamics. Proc. R. Soc. A **463**, 855–880 (2007)
13. Pendry, J.B.: Negative refraction makes a perfect lens. Phys. Rev. Lett. **85**, 3966–39669 (2000)
14. Smith, D.R., Pendry, J.B., Wiltshire, M.C.K.: Metamaterials and negative refractive index. Science **305**, 788–792 (2004)
15. Sihvola, A.: Metamaterials in electromagnetics. Metamaterials **1**, 2–11 (2007)
16. Shamonina, E., Solymar, L.: How the subject started metamaterials. Metamaterials **1**, 12–18 (2007)
17. Sheng, P., Mei, J., Liu, Z.Y., Wen, W.J.: Dynamic mass density and acoustic metamaterials. Phys. B **394**, 256–261 (2007)
18. Zhou, X.M., Hu, G.K.: Analytic model of elastic metamaterials with local resonances. Phys. Rev. B **79**, 195109 (2009)
19. Zhu, R., Huang, H., Huang, G.L., et al.: Microstructure continuum modeling of an elastic metamaterial. Int. J. Eng. Sci. **49**, 1477–1485 (2011)